

Supporting Information

Accelerated Reactions of Amines with Carbon Dioxide Driven by Superacid at the Microdroplet Interface

Kai-Hung Huang, Zhenwei Wei and R. Graham Cooks*

Department of Chemistry, Purdue University, West Lafayette, Indiana 47907, United States

e-mail: cooks@purdue.edu

Table of Contents

1. Experimental procedure and general information.....	S2
2. Amine reactions with CO₂ using room air: effect of basicity and sterics.....	S5
3. Amine reactions with CO₂ using room air: effect of concentration and pH.....	S8
4. Effect of deliberate addition of CO₂ into amine solution.....	S10
5. Addition of CO₂ at the droplet interface and analysis by ESSI.....	S12
6. Summary of the amine/CO₂ reaction under different conditions.....	S25
7. The possibility of gas phase ion/molecule reactions	S27
8. References.....	S31

1. Experimental procedure and general information

(1) Materials

Amines listed in **Scheme S1** and **Table S1** were purchased from Sigma-Aldrich while acetonitrile (ACN) was purchased from Fisher Scientific. Hydrochloric acid solution (36.5% - 38.0%) was purchased from Avantor Performance Materials.

(2) Amine reaction with room air CO₂ (effect of basicity, sterics, concentration and pH)

Amines were dissolved in ACN at a concentration of 10 mM, and then diluted to the desired concentration (10 μ M, 100 μ M and 1000 μ M) for subsequent experiments. To study the effect of pH, three samples were prepared by adding to 1 mL of DBPA solution in ACN (i) 10 μ L hydrochloric acid (35%) (ii) 5 μ L HCl and 5 μ L ACN and (iii) 10 μ L ACN to amine solution to serve as control. For all the experiments (different amines, concentration dependence, and pH-dependence), amine solutions were loaded into a nESI capillary (5 μ m tip inner diameter as estimated using a Konus Campus Binocular microscope) and sprayed for droplet reaction and mass analysis. The distance between nano tip and the inlet of the mass spectrometer was 4 +/- 1 mm.

(3) Deliberate addition of CO₂ into solution in three ways

Amine solutions were prepared by the previous procedure (with 20mM in the bicarbonate case and 10 mM in the dry ice and bubbling CO₂ cases). (i) Sodium bicarbonate was dissolved into ACN to create a saturated solution which was mixed with an equal volume of the amine solution. (ii) Dry ice was added to the amine solution (2 mL) and the vials were sealed after the weight of the solution had increased by 0.050 g upon adding dry ice. (iii) CO₂ gas was injected into the solution using PEEK tubing (125 μ m O.D.) for 10 seconds (under 20 psi), and then the vials were sealed before analysis. After treatment in these three ways, the solutions were analyzed using the same nESI procedure described above. We also used ESSI as the ionization method for case (iii), as discussed below.

(4) Addition of CO₂ in the gas phase as nebulizing gas

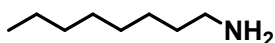
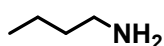
Amine solutions, as well as amine solutions with injected CO₂, were prepared as previously mentioned, and droplet reaction/analysis was performed by ESSI-MS. A homemade source was used to perform ESSI using CO₂ as the nebulizing gas. The capillary (I.D./O.D.=250 μ m/350 μ m) used to inject the amine solution was connected to a 500 μ L syringe (Hamilton) and a flowrate of 5 μ L/min was used. The amine solution was sprayed with nebulization by CO₂ gas under 120 psi. For comparison, the amine solution containing injected CO₂ was sprayed using N₂ under the same pressure. The distance between the tip of the capillary and the inlet of the mass spectrometer was about 2 cm. In the special case of distance-dependent experiments this was varied from 2 mm to 20 mm.

Primary amine	Positive (<i>m/z</i>)	Negative (<i>m/z</i>)	Dominant*
Butylamine	74.09	116.09	V
Octylamine	130.18	172.18	V
tert-octylamine	130.18	NA	NA

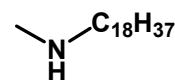
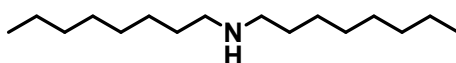
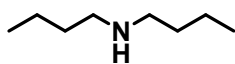
(5) Mass spectrometer parameters

nESI-MS and ESSI-MS were performed using an LTQ mass spectrometer (ThermoFisher Scientific, San Jose, California) in both the positive ion and negative ion modes. A high voltage (1.5kV for nESI and 4.5 kV for ESSI) was applied *via* an alligator clip onto the wire of nano tip holder (nESI) or the needle of the syringe (ESSI). The ion sources parameters were set as follows: capillary voltage: +15 V, capillary temperature: 250 °C, tube lens voltage: +65V.

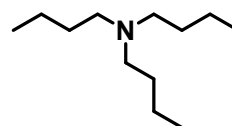
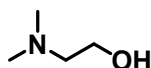
Primary amines



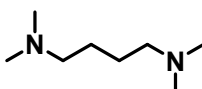
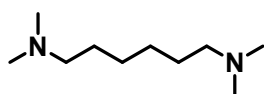
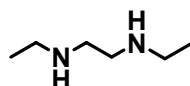
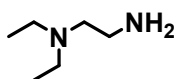
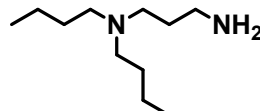
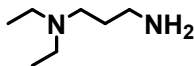
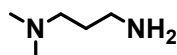
Secondary amines



Tertiary amines



Diamines



Scheme S1. Amines used in this study

Secondary amine	Positive	Negative	Dominant
Dibutylamine	130.18	172.18	X
Diocetylamine	242.45	284.36	V
N-methyloctadecyl amine	284.55	326.45	X
Tertiary amine	Positive	Negative	Dominant
N,N-dimethylethanoamine	90.09	132.09	X
N,N-dimethylethelamine	74.09	NA	NA
Tributylamine	186.27	NA	NA
Diamine	Positive	Negative	Dominant
N,N-Dimethyl-1,3-propanediamine	103.09	145.09	V
N,N-Diethyl-1,3-propanediamine	131.18	173.18	V
N,N-Dibutyl-1,3-propanediamine	187.27	229.27	V
N,N-Diethylethylenediamine	117.18	159.18	V
N,N'-Diethylethylenediamine	117.18	159.18	V
N,N,N',N'-tetramethyl-1,6-hexanediamine	173.27	NA	NA
N,N,N',N'-tetramethyl-1,4-butanediamine	145.18	NA	NA

Table S1. Amines used in this study and summary of MS data for protonated amines and carbamate anions

* The column titled "positive" lists the detected m/z of protonated amine species

* The column titled "negative" lists the m/z of carbamate anion

* V indicates that the carbamate anion is a dominant feature in the negative ion spectrum; while X means the carbamate anion is not a dominant feature. NA means no $[M+43]^-$ is detected in negative ion mode

2. Amine reactions with CO₂ using room air: effect of basicity and sterics

To investigate the effect of basicity and sterics on the reactions of amines with room air CO₂, we sprayed the amine by nESI without using any additional CO₂ source. Various amines were tested, with t-octylamine representing an extreme case of steric hindrance. Consistent with the results for DBPA (**Figure S1**), the protonated species [M+1]⁺ were observed in the positive mode, while the carbamate anions [M+43]⁻ were detected in the negative mode. For the primary amines and those diamines with one primary amine group, the carbamate anion [M+43]⁻ was a dominant feature of the negative ion spectra. (**Figure S2a-c and 2j-l**). Note that carbamate anions were not detected for tert-octylamine, presumably for steric reasons. Even though [M+43]⁻ ions were detected in the negative mode when spraying secondary amines (**Figure S2d-f**), they were of low abundance, suggesting that the increased basicity of secondary amines is offset by higher steric hindrance. The [M+43]⁻ species were not detected for the diamines which contained tertiary amine groups (**Figure S2h-i and 2n-o**), indicating a dominant role of steric hindrance in these cases. However, the tertiary amine N,N-dimethylethanoamine (**Figure S2g**), did react at the hydroxyl group as seen by comparing the spectrum with that of N,N-dimethylethylamine (**Figure S2h**). The formation of carbamate depends on not only the basicity of the nucleophile but also on steric effects.

Moreover, we implemented tandem mass spectrometry to validate the structures of [M+43]⁻, which on this basis we confirmed to be the carbamate anion. All the MS/MS spectra shown were recorded using CID energy of 30. The fragmentations seen are readily explained although the loss of formic acid (46 Dalton) and the associated loss of 48 Da (additional H₂ elimination) are interesting for their putative formation of carbanions stabilized by imines)

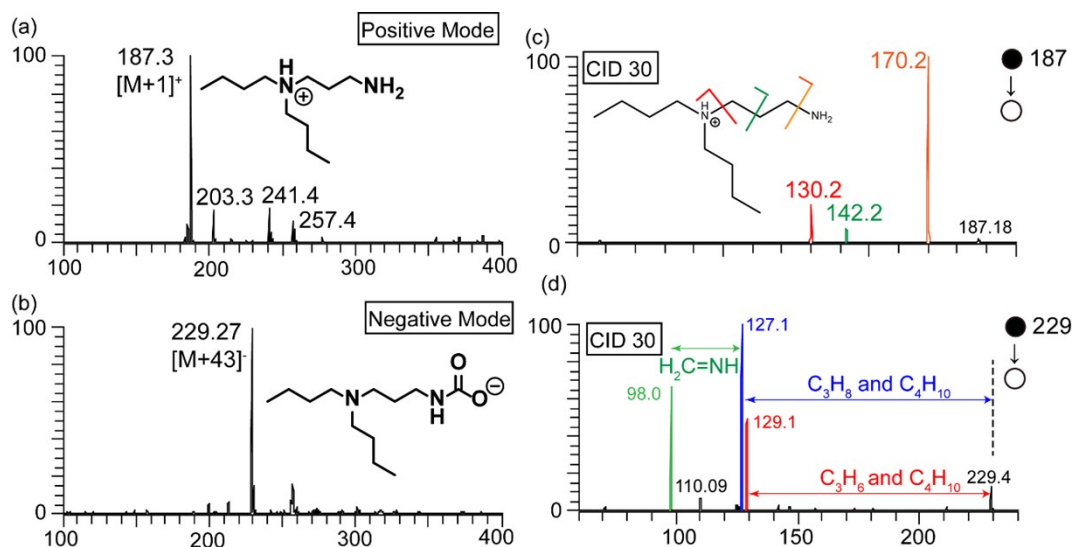


Figure S1. Reaction of DBPA with room air CO₂. Spraying DBPA (10 mM) using nESI with detection in (a) positive and (b) negative ion mode. Tandem mass spectra of (c) *m/z* 187

(protonated DBPA) and (d) m/z 229 (carbamate anion). Nominal collision energy is 30 arb. units.

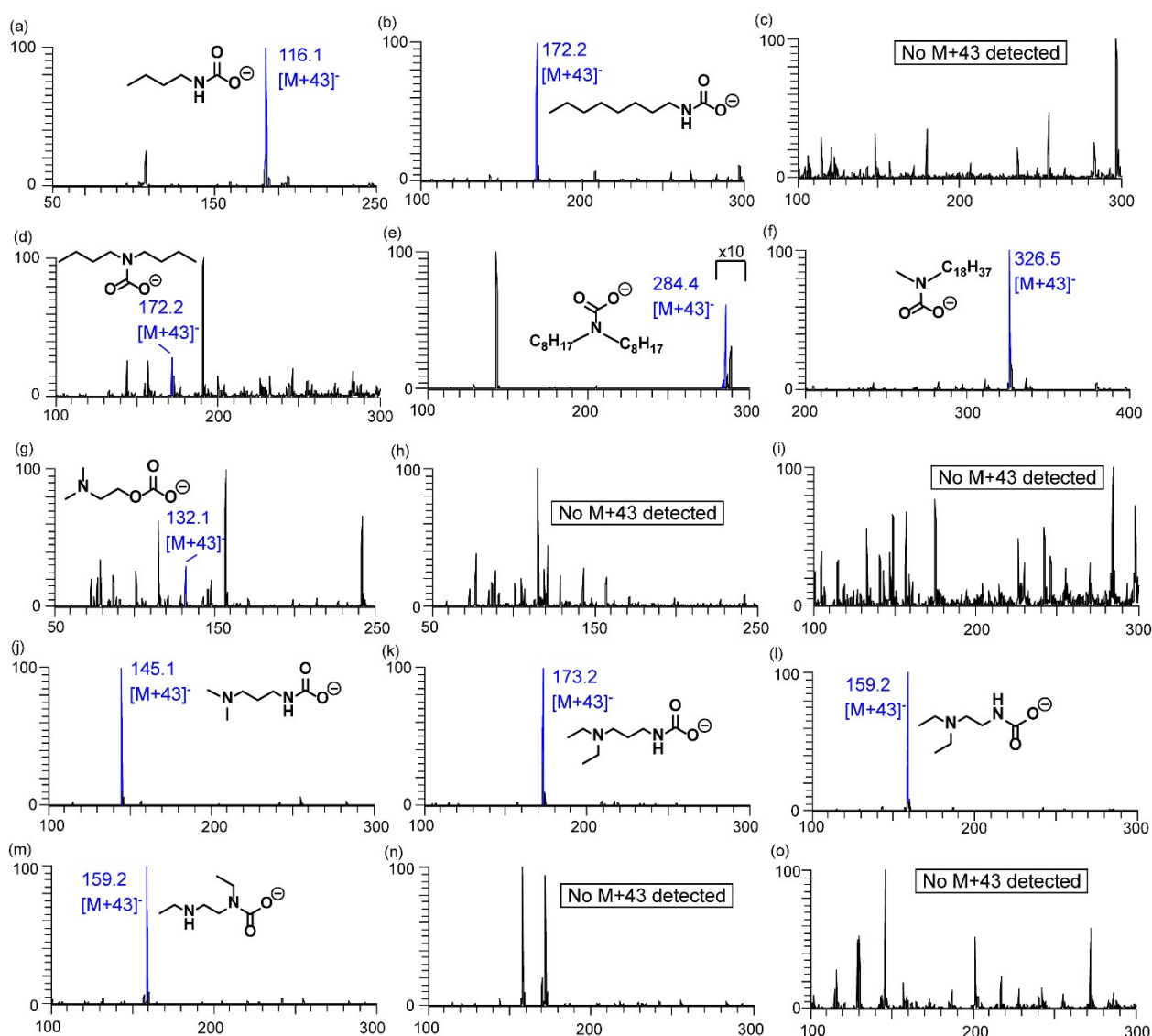


Figure S2. Effect of basicity and sterics with room air CO_2 . Mass spectra recorded when spraying amines (10 mM) using nanoESI and detecting in negative modes. (a) Butylamine (b) Octylamine (c) tert-octylamine (d) Dibutylamine (e) Dioctylamine (f) N-methyloctadecylamine (g) N,N-dimethylethanoamine (h) N,N-dimethylethelamine (i) Tributylamine (j) N,N-Dimethyl-1,3-propanediamine (k) N,N-Diethyl-1,3-propanediamine (l) N,N-Diethylethylenediamine (m) N,N'-Diethylethylenediamine (n) N,N,N',N'-tetramethyl-1,6-hexanediamine (o) N,N,N',N'-tetramethyl-1,4-butanediamine

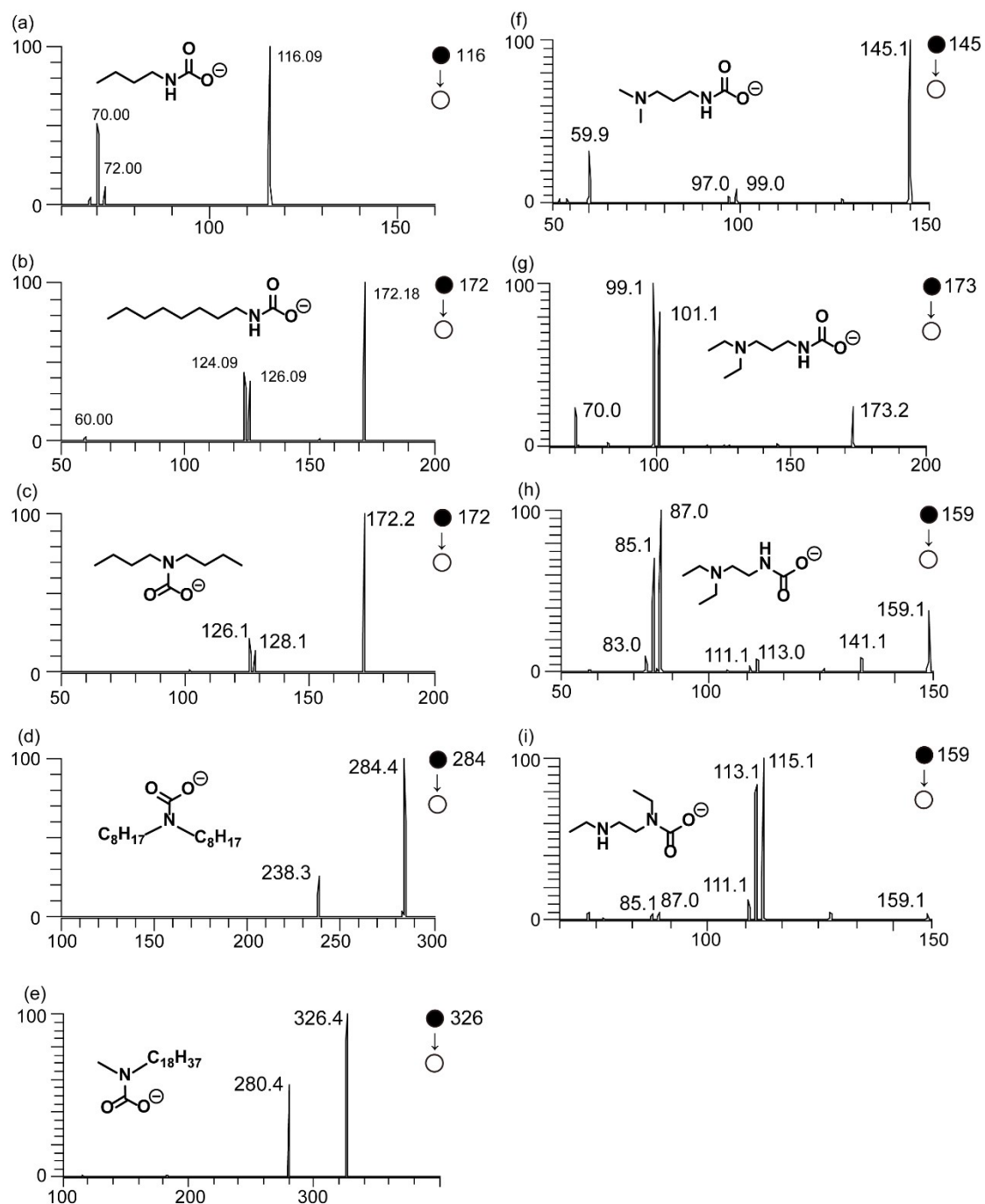


Figure S3. Verification of carbamate anion. MS/MS of carbamate anion detected when spraying amines in room air. MS/MS spectrum of (a) butylamine (b) octylamine, (c) dibutylamine (d) dioctylamine, (e) N-methyloctadecyl amine, (f) N,N-Dimethyl-1,3-propanediamine, (g) N,N-Diethyl-1,3-propanediamine, (h) N,N-Diethylethylenediamine and (i) N,N'-Diethylethylenediamine Fragmentations are explained in the text.

3. Amine reactions with CO₂ in room air: effect of concentration and pH

We investigated the effect of amine concentration and pH value on the formation of carbamate anions in room air spray experiments. As the concentration of amine was raised, the positive ion spectra did not change significantly, however, the signal intensity of carbamate anion and its signal to noise ratio increased greatly. (**Figure S4**) (Note that the conversion ratio did not increase.) This is simply attributed to the generation of more carbamate by the concentrated amine. Additionally, **Figure S5** shows the effect of changing pH by the addition of HCl. Protonated species $[M+1]^+$ remained the dominant peak in the positive mode after adding HCl, while the carbamate ($M+43$) decreased dramatically in the negative mode. Moreover, we could hardly observe the carbamate species in the negative mode, while the species corresponding to $[\text{amine}+\text{HCl}+\text{Cl}]^-$ became dominant in the negative ion mode when the amount of HCl was increased. These results suggest that adding acid in the solution impedes the reaction between the amine group and carbon dioxide by decreasing the nucleophilicity of the amine group.

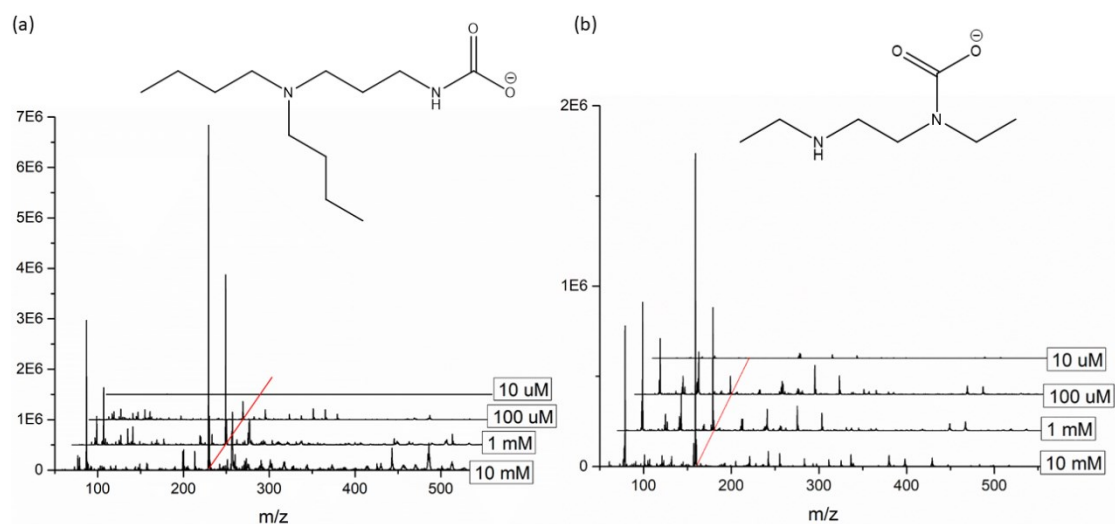


Figure S4. Concentration effect for amine/room air CO₂ reactions. Concentration dependence of carbamate of (a) DBPA and (b) N,N'-diethylethylenediamine in the negative ion mode using nanoESI.

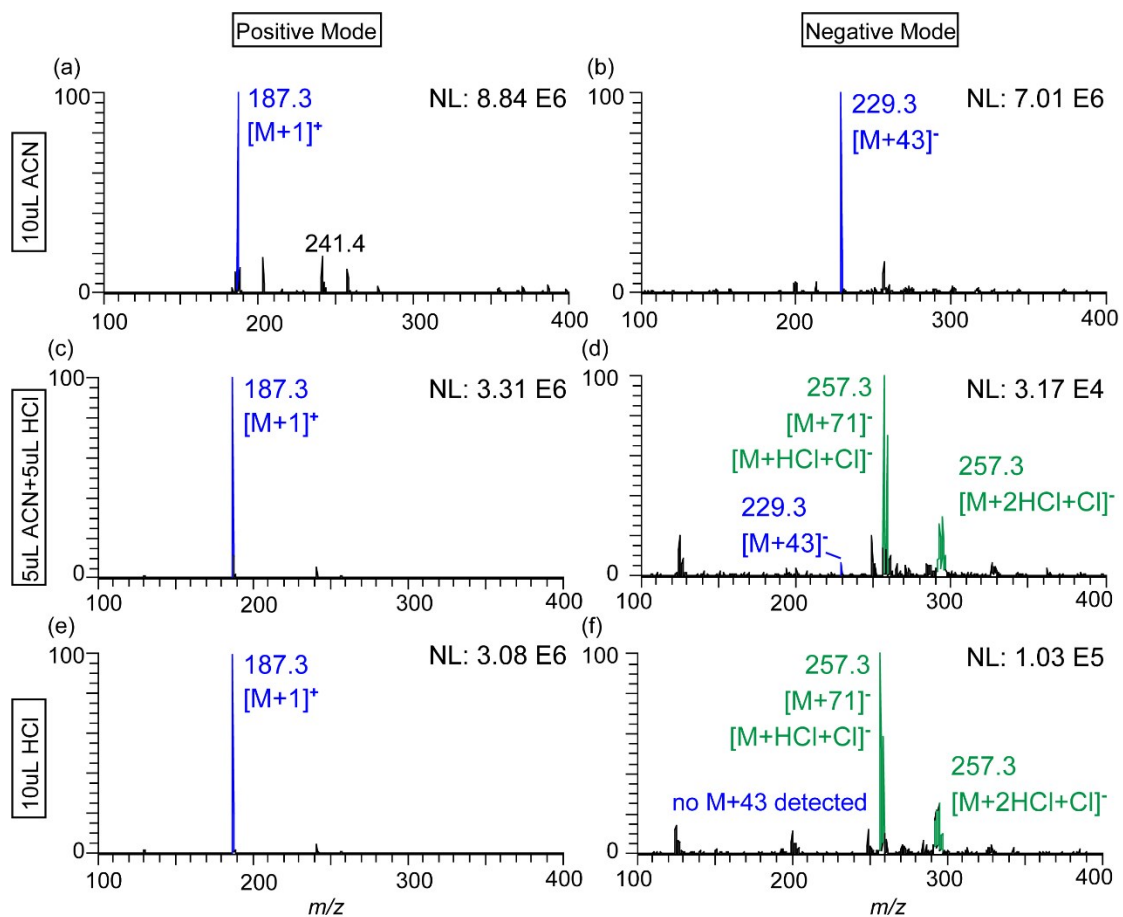


Figure S5. pH effect for amine/room air CO₂ reactions. Mass spectra of DBPA recorded in room air before and after adding 35% HCl in the proportions indicated.

4. Effects of deliberate addition of CO₂ into amine solution

Deliberate addition of CO₂ gives results that differ from those seen when reaction is with room air CO₂. In these experiments we intentionally added CO₂ into the amine solution to promote reaction.

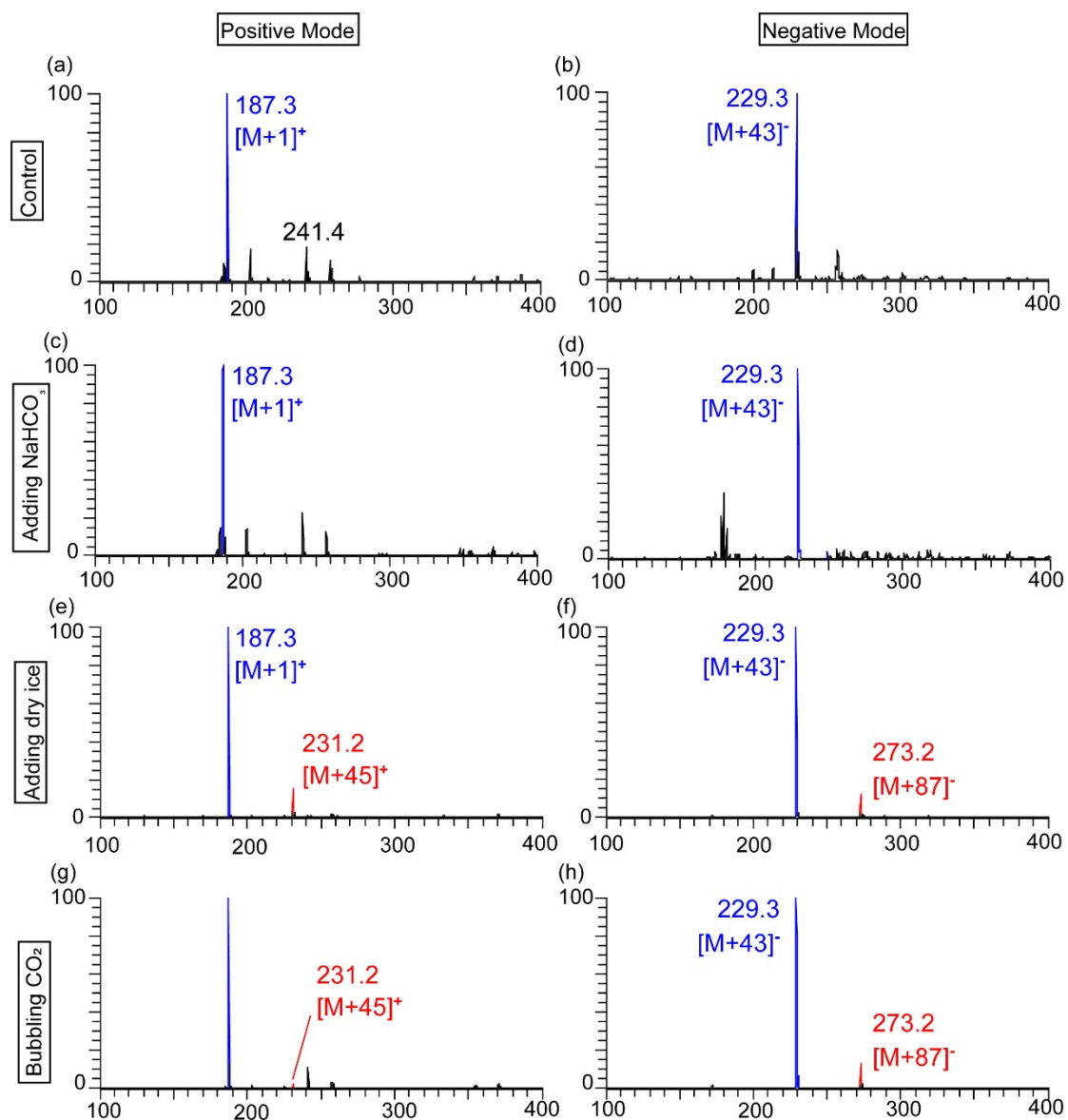


Figure S6. Effect of deliberate addition of CO₂ into the amine solution. Positive and negative ion nESI spectra of DBPA solutions to which CO₂ had been added using the CO₂ sources shown.

The MS/MS of two amine carbamates (*m/z* 231 and *m/z* 273) are shown in Figure S7.

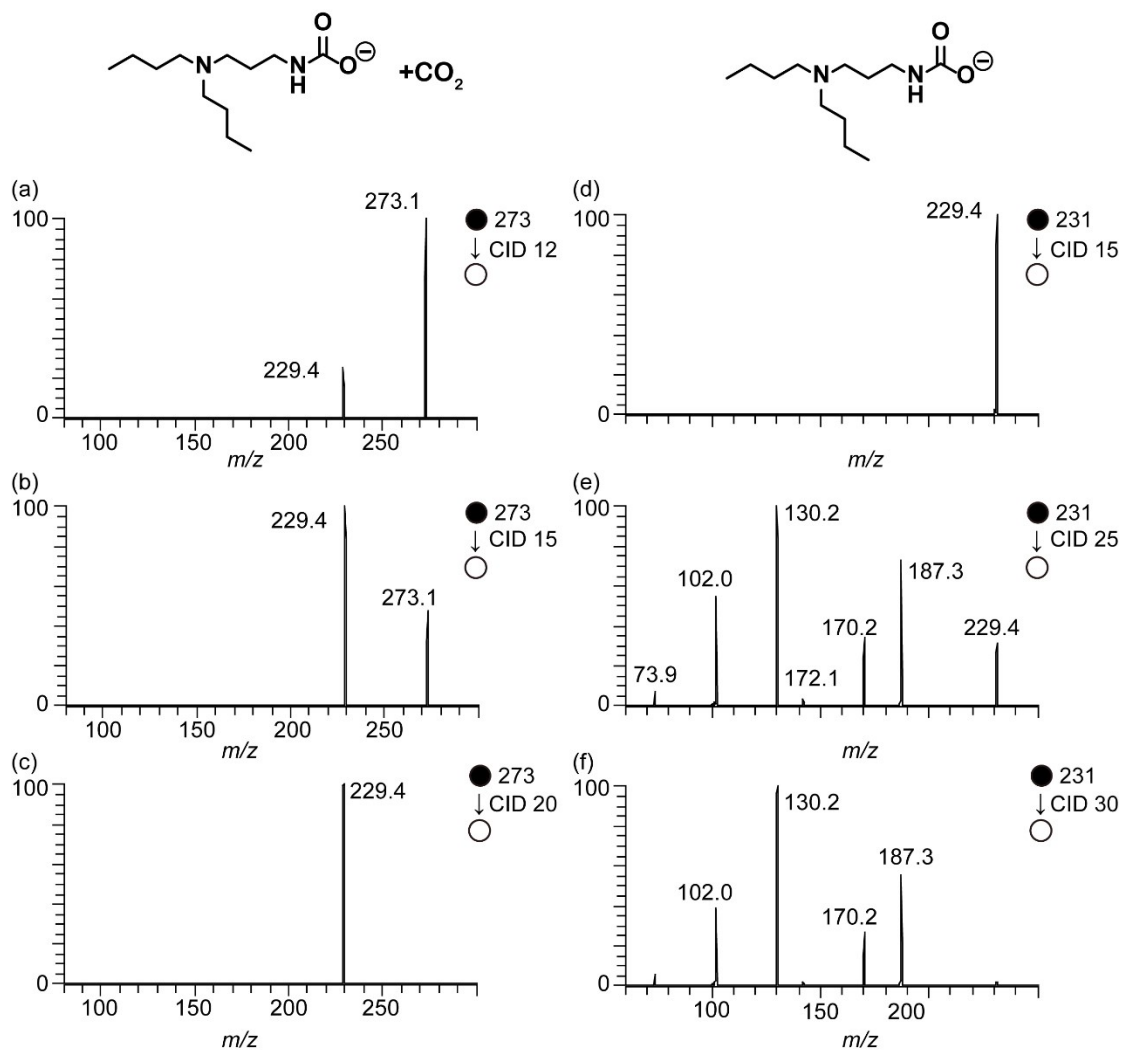


Figure S7. Tandem mass spectra of species found after deliberate addition of CO₂ into the DBPA solution. MS/MS of m/z 273 and m/z 231 under different collision energies. For annotation of the fragments of m/z 231 please refer to Figure 1 (main text).

5. Addition of CO₂ at the droplet interface and analysis by ESSI

In this section, we intentionally added CO₂ in the gas phase (by utilizing it as nebulization gas) to promote interfacial reactions with amine-containing droplets. Control experiments utilized N₂ as nebulization gas. This approach is different to the one in which CO₂ was injected into solution by (i) short reaction time and (ii) the interfacial nature of the reaction. Implementing ESSI ensures that the reaction only happens after the generation of droplets, and the reaction time can be considered as the flight time of the droplets which depends on the distance between the tip of the sprayer to the inlet of mass spectrometer. This reaction time is estimated (see next paragraph) to be in the range 0.17 - 0.33 ms.¹ The injection of CO₂ into the solution results in what can be considered as a bulk reaction and the ESSI experiment is considered as a droplet reaction. Evidence that reaction occurs during the flight of droplet is given in **Fig. 2** and **Figs. S8-9** as well as in section 7.

To establish whether the droplet reaction is truly and only interfacial, we can (roughly) estimate the thickness of the reaction region (which is determined by the diffusion length of CO₂ into acetonitrile). The diffusion coefficient was estimated to be ca. $1 \times 10^{-9} \text{ m}^2\text{s}^{-1}$.^{1,2} From Fick's second law of diffusion, we can calculate the diffusion length from the diffusion coefficient and diffusion time (0.2 ms). This gives a diffusion length in ESSI of 0.63 μm which corresponds to the surface region of the droplet generated by ESSI (size estimated as ca. 3 - 6 μm).⁴⁻⁶ Therefore, the microdroplet reaction can be considered as interfacial reaction rather than reaction occurring throughout the droplet.

To compare the effect of providing CO₂ in the gas phase (at the interface) and from the solution, we conducted an experiment in which CO₂ was bubbled into the solution which was then sprayed by N₂ using ESSI. Gaseous CO₂ was injected into a DBPA solution (in ACN) via PEEK tubing for 10 seconds and then the solution was immediately analyzed by ESSI. The CO₂ can be considered as being in excess and uniformly distributed throughout the solution in this case, and the difference between this experiment and the similar experiment in section 4 is that the analytical method here is ESSI for better comparison with the CO₂ nebulization experiment, viz. the interfacial droplet reaction. A detailed explanation and comparison of the results when CO₂ is supplied from gas phase and from solution is given in the main text.

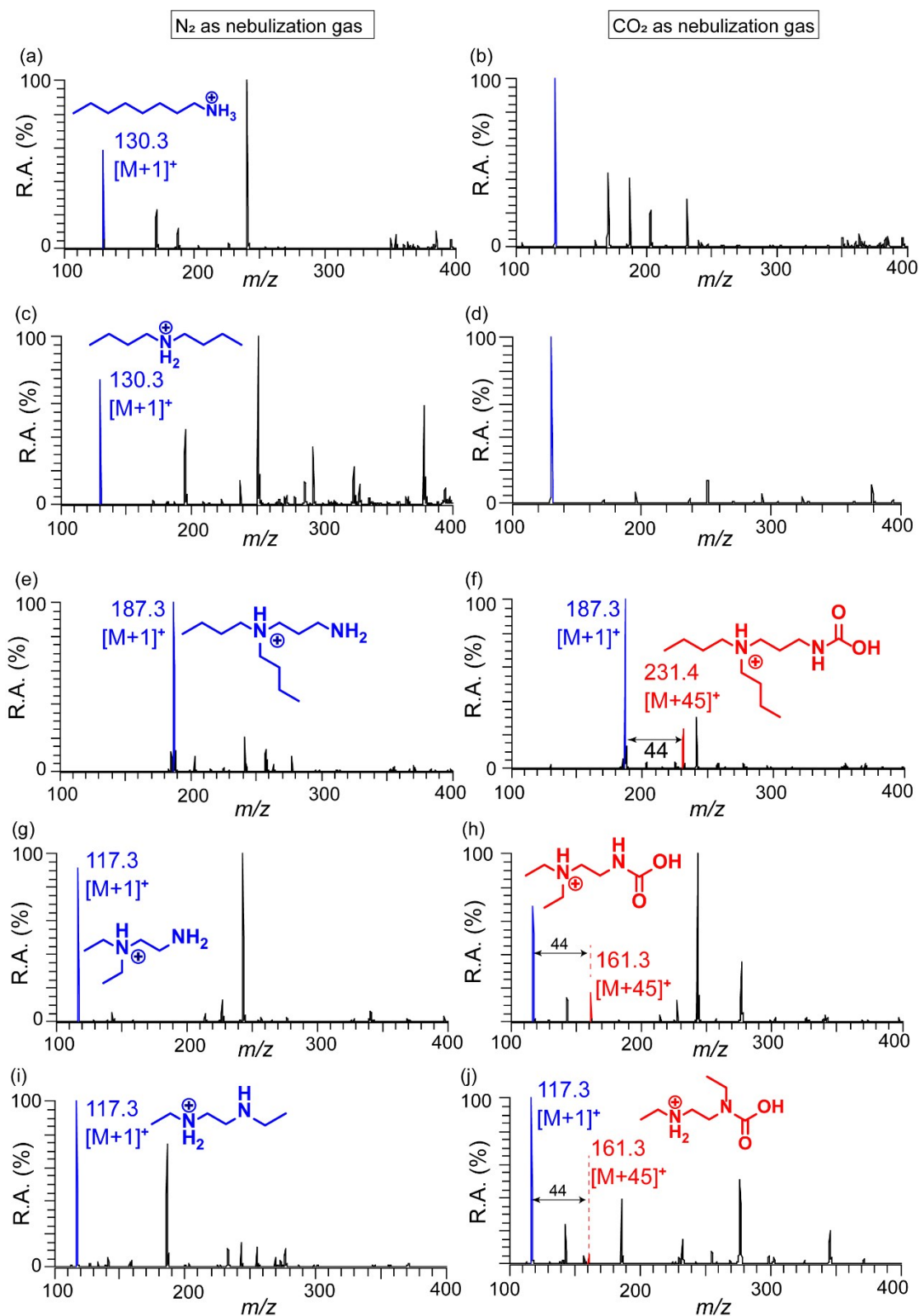


Figure S8. Amine droplet/CO₂ vapor reaction in positive mode. Mass spectra recorded using N₂ and CO₂ as ESSI nebulization gas for representative amines (1000 μM) listed in main text.

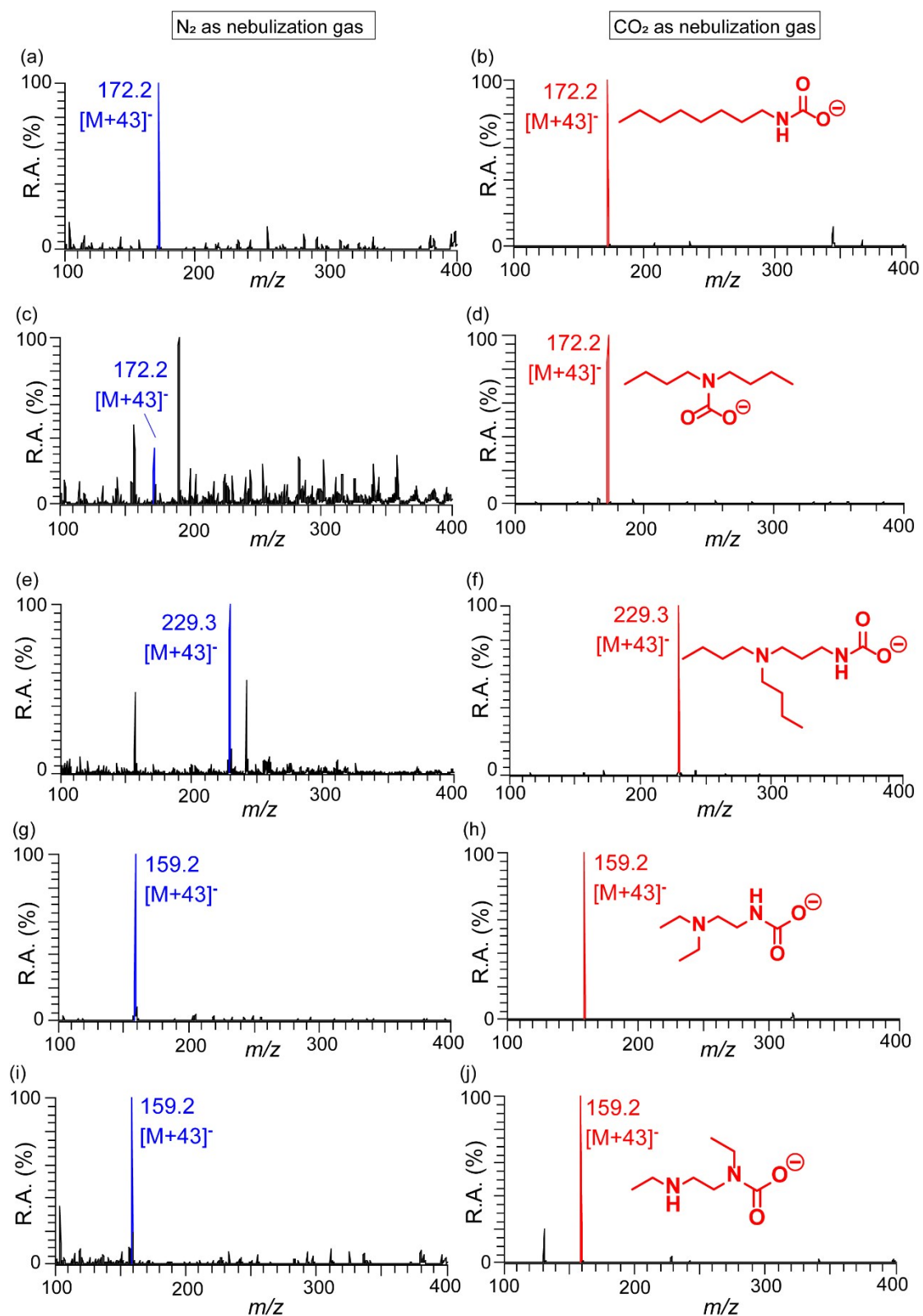


Figure S9. Amine droplet/CO₂ vapor reaction in negative mode. Mass spectra recorded using N₂ and CO₂ as nebulization gas in ESSI for five representative amines (1000 μM).

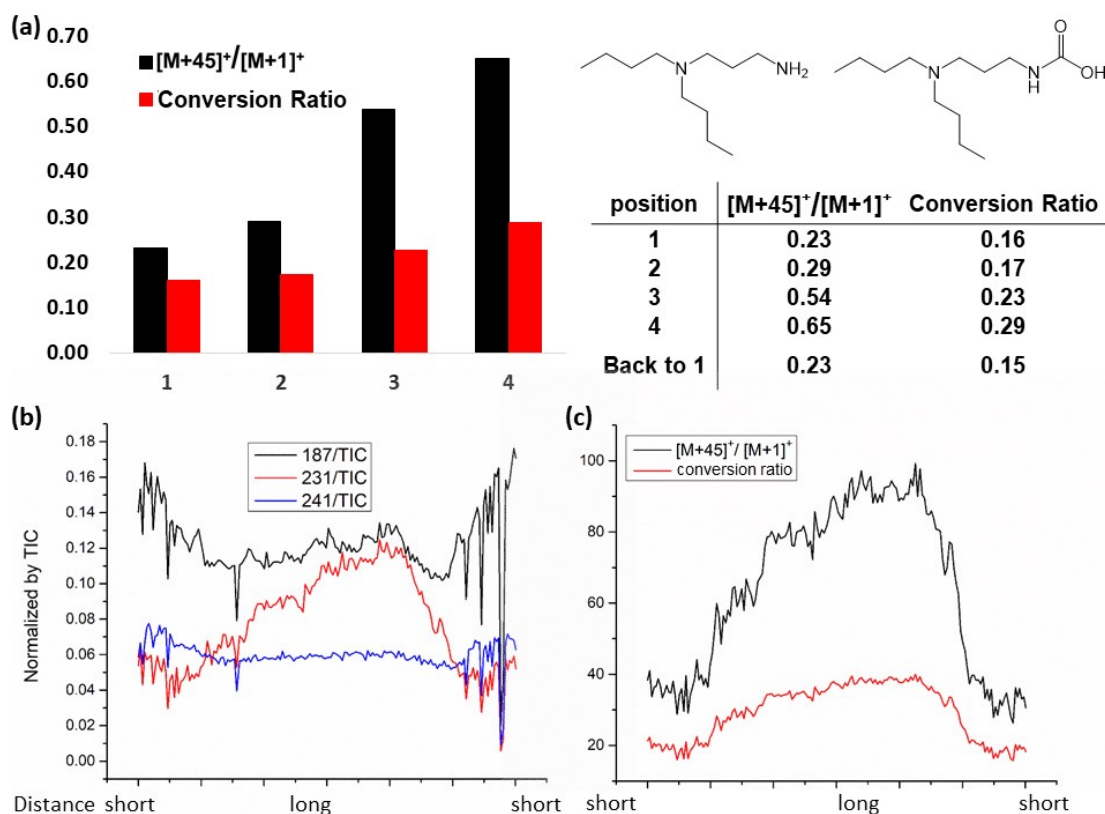


Figure S10. Distance effect in amine droplet/CO₂ vapor reaction. Distance dependent experiment for N,N-di-nbutyl-1,3-propylenediamine (DBPA) (10 μ M in ACN) in the positive ion mode. The $[M + 45]^+$ and $[M + H]^+$ ions occur at m/z 231 and m/z 187, respectively. (a) Static experiment: sprayer and the inlet of mass spectrometer were set at position 1 to 4 corresponding to an increased distance between them. (b) and (c) Dynamic experiment: distance between the sprayer and the inlet of mass spectrometer was varied continuously using a moving stage. Note that 'short' corresponds to 2 mm and 'long' corresponds to 30 mm. The stage was moved backward and then forward, increasing and then decreasing the distance. The ion m/z 187 is protonated DBPA (reagent); m/z 231 is protonated carbamic acid. Note that the ion m/z 241 represents starting material; MS/MS interpretation is given in **Fig. S12**.

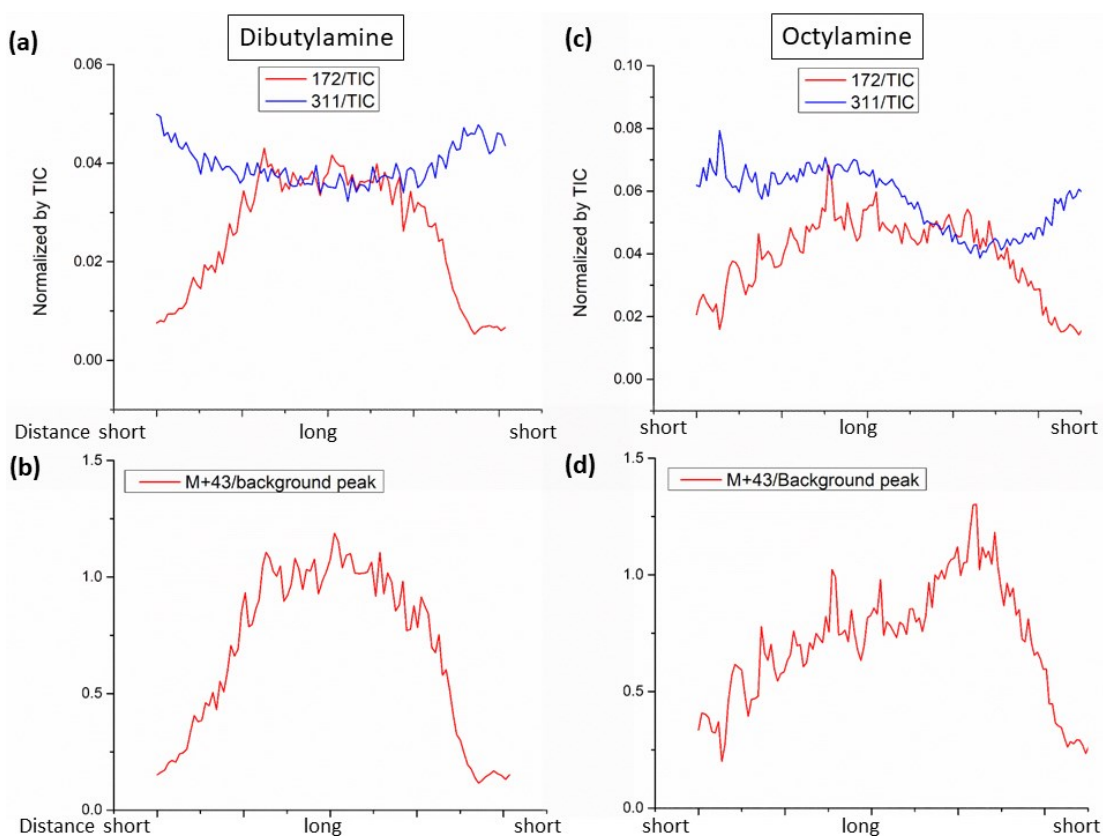


Figure S11. Distance effect of amine droplet/CO₂ vapor reaction. Distance-dependence experiment of (a), (b) dibutylamine and (c), (d) octylamine in negative mode. Distance between the sprayer and the inlet of mass spectrometer was varied using a moving stage (the short distance corresponds to 2 mm and the long distance to 20 mm). The stage was moved backward and then forward, making the distance longer and then shorter, while recording the data. Signals are given as ratio against total ion current (TIC) or background peak (m/z 311).

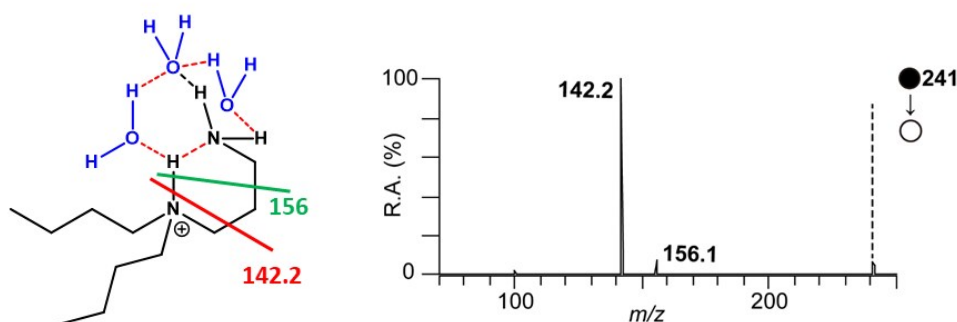


Figure S12. Characterization of m/z 241. MS/MS spectrum of this DBPA ion, proposed to be a trihydrate with a triple six-membered ring structure. (Spraying DBPA in ACN under ambient conditions generates an abundant ion species corresponding to m/z 241.) The relatively stable tris-six membered ring structure appears to favor the generation of this ion/molecule cluster. The water molecules may be captured from the ambient humidity or from impurity in solvent.

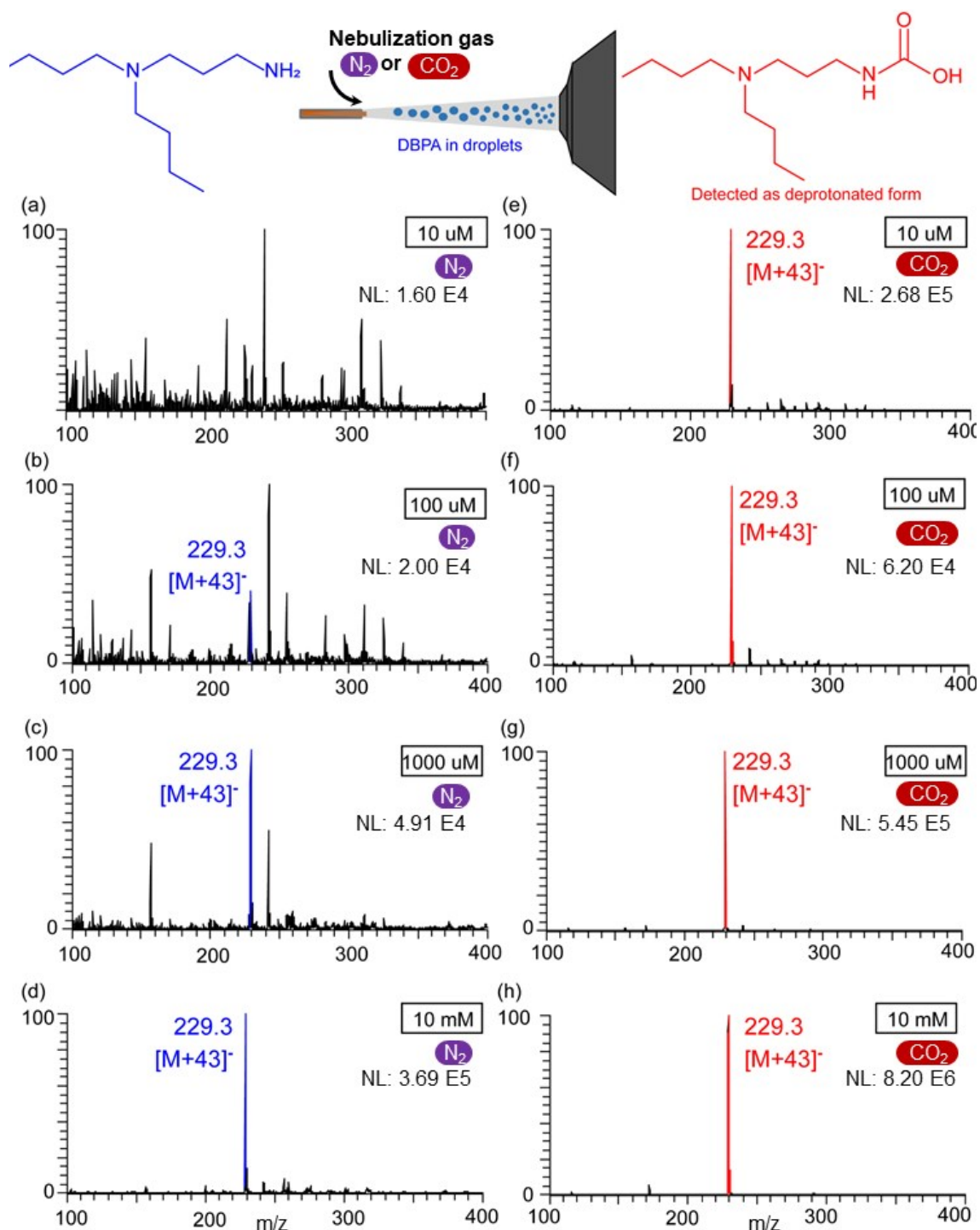


Figure S13 Amine droplet/ CO_2 vapor reaction and control experiment. EESI of DBPA using N_2 (control) or CO_2 (droplet reaction) as nebulization gases with different amine concentrations (negative mode)

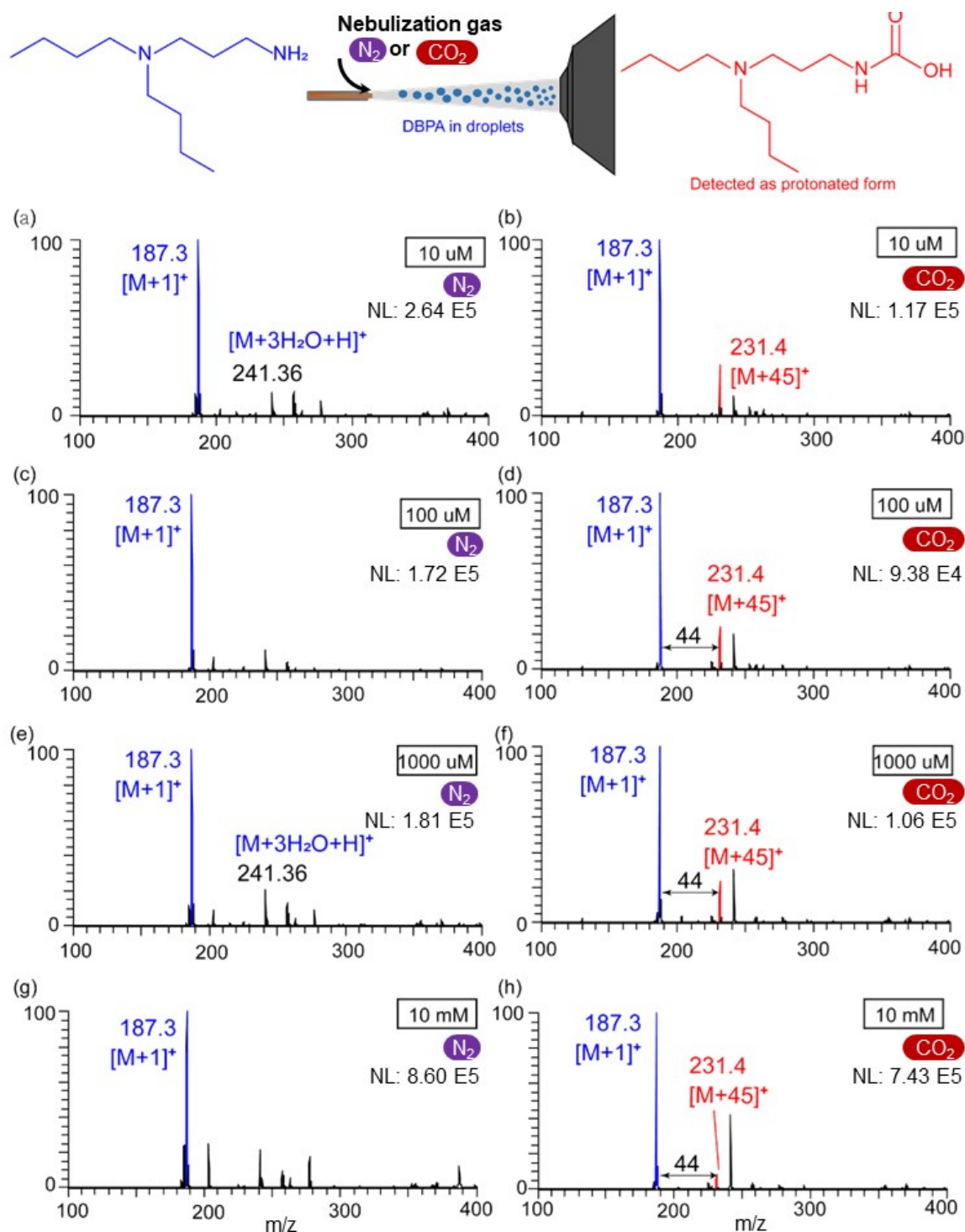


Figure S14. Amine droplet/CO₂ vapor reaction and control experiment. EESI of DBPA using N₂ (control) or CO₂ (droplet reaction) as nebulization gases with different amine concentrations (positive mode).

Table S2. Amine concentration effect in DBPA droplet/CO₂ vapor reactions examined in positive mode^a

[Amine] (uM)	Log[amine]	[M+45] ⁺ /[M+1] ⁺ (Triplicate)			Avg	Std
10	1.0	30.8	51.8	36.0	39.5	9.0
100	2.0	16.7	18.6	16.7	17.3	0.9
500	2.7	19.1	16.4	17.0	17.5	1.1
1000	3.0	16.2	15.8	13.9	15.3	1.0
5000	3.7	11.6	8.93	8.84	9.81	1.30
10000	4.0	4.14	7.27	5.63	5.68	1.28

^aRatio [M+45]⁺ (protonated carbamic acid, product) to [M+1]⁺ (starting material) at different amine concentrations using CO₂ assisted ESSI. Triplicate determinations are listed.

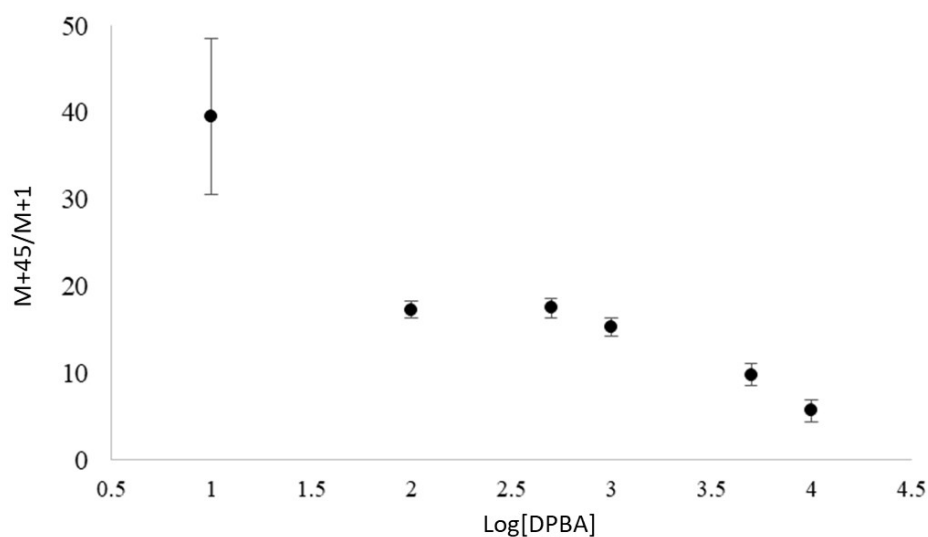


Figure S15. Concentration effect of amine/CO₂ droplet reaction. Concentration dependence of reaction of DBPA and CO₂ using ESSI.

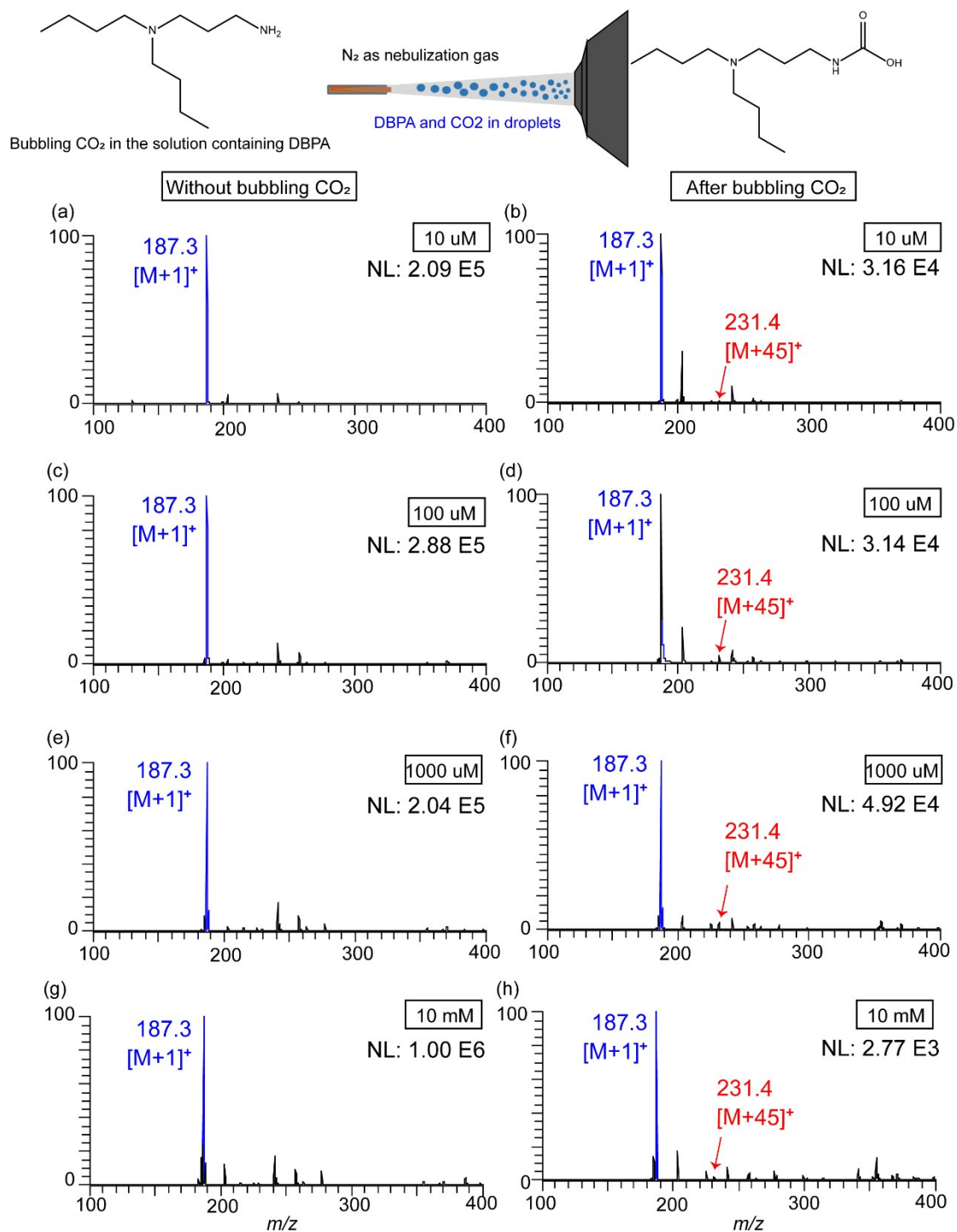


Figure S16. Reaction of CO₂ in solution and then using N₂ as nebulization gas to record positive ion mode EESI.

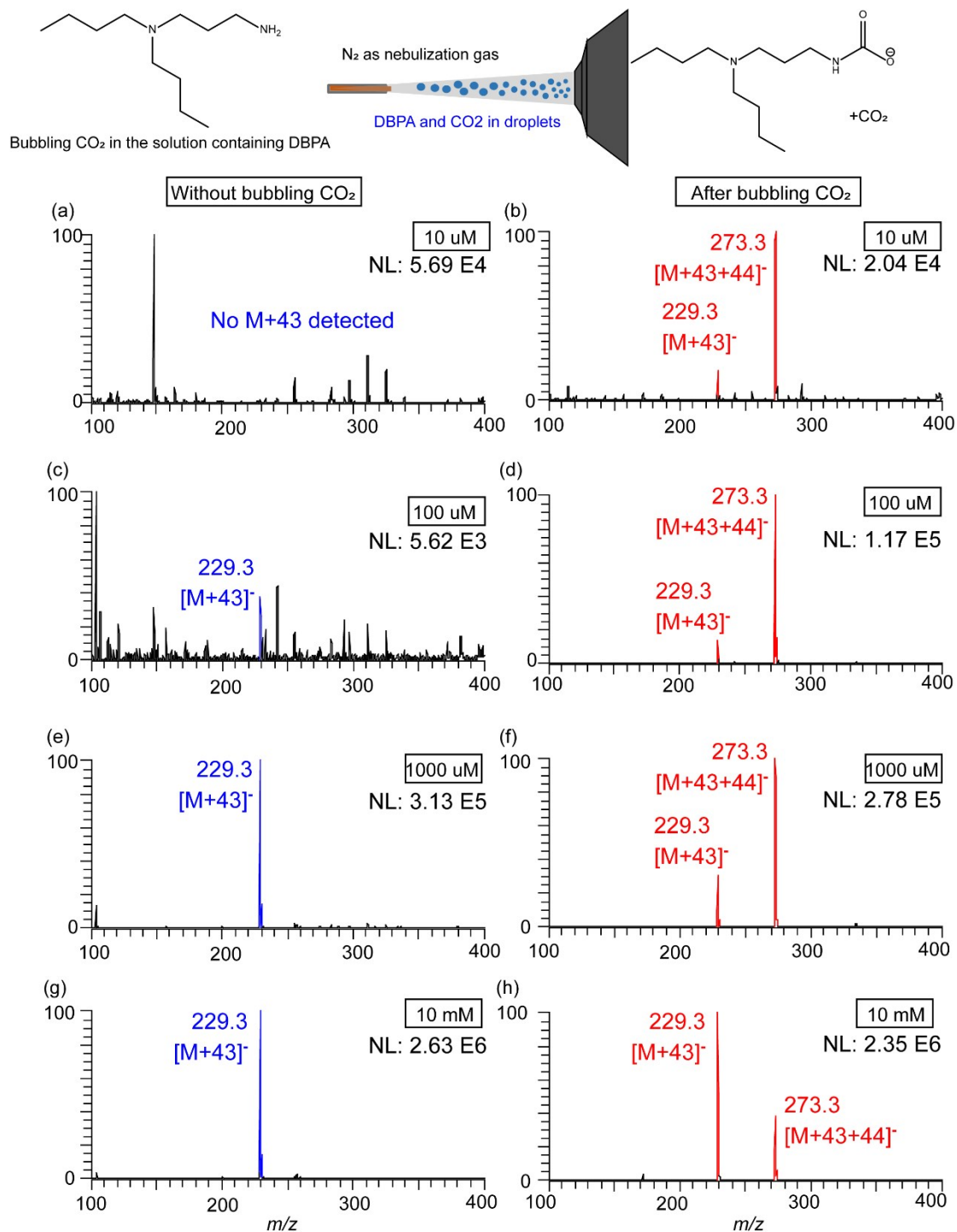
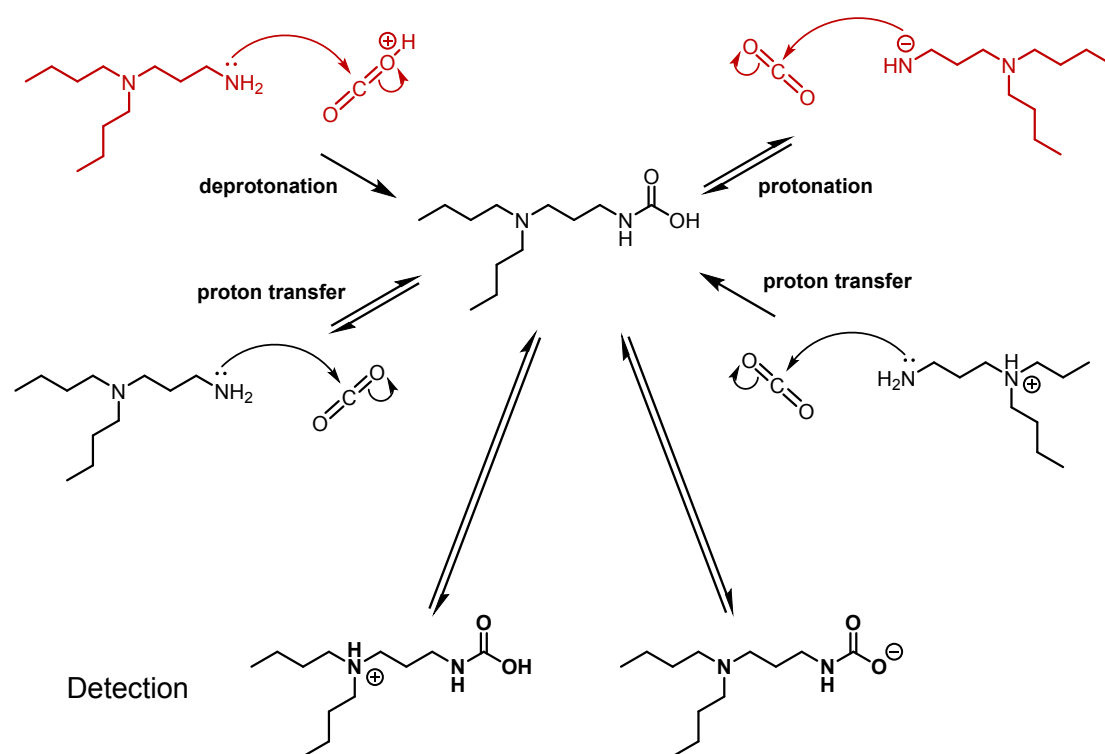


Figure S17. Reaction of CO₂ injected into a solution and then using N₂ as nebulization gas to record negative ion mode EESI.

Scheme S2. Mechanism Suggested mechanism for carbamic acid formation showing the ionic species used for its detection in the positive and negative modes



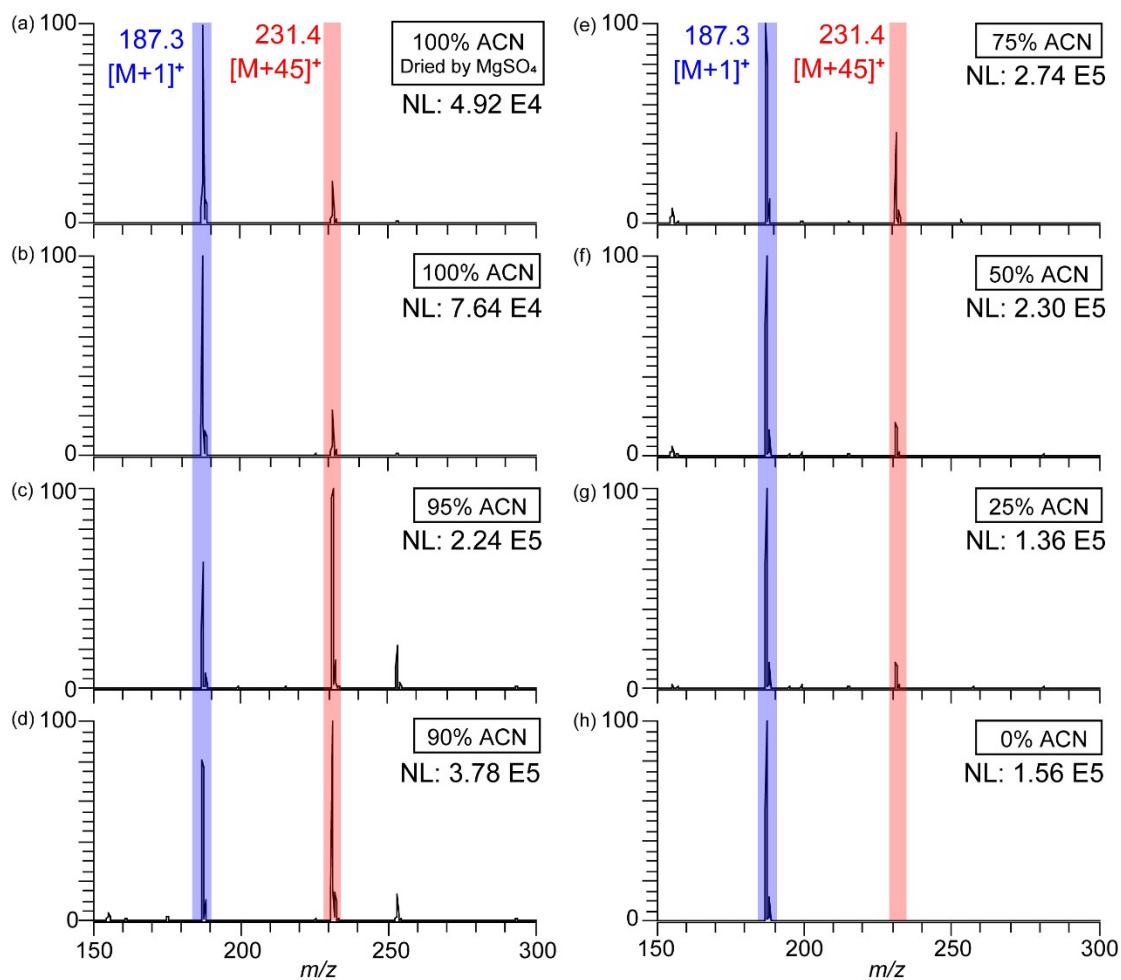
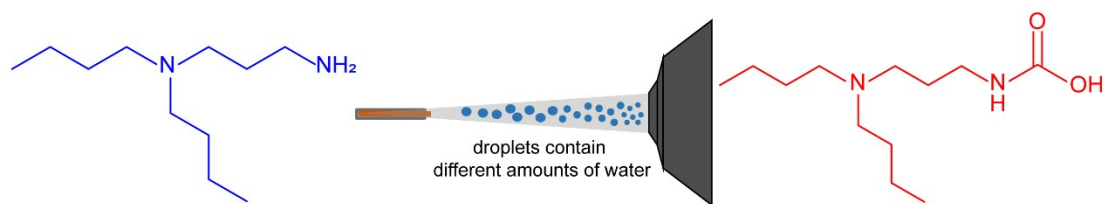


Figure S18. Effect of trace amounts of water. Spectra recorded using solvents of different compositions as listed. Note that 100% ACN means that the ACN was treated with drying agent (MgSO₄), however, the room humidity was not eliminated in this case. The 99% case is for ACN taken directly from the commercial container, which contains a small amount of water as impurity.

Table S3. Effect of trace amounts of water^a

% of ACN	Conversion Ratio			average	std
	#1	#2	#3		
0	0.26	0.24	0.65	0.38	0.23
25	3.00	12.59	11.91	9.17	5.35
50	10.77	14.68	15.06	13.50	2.38
75	31.52	32.32	31.65	31.83	0.43
90	59.81	53.75	55.62	56.39	3.10
95	61.22	58.67	60.24	60.04	1.29
100% ACN Not dried by MgSO ₄	19.54	17.37	18.53	18.48	1.09
100% ACN Dried by MgSO ₄	22.03	17.15	17.55	18.91	2.71

^a Conversion ratios calculated for triplicate composition-dependent experiments

% ACN is calculated from the % volume mixed with H₂O

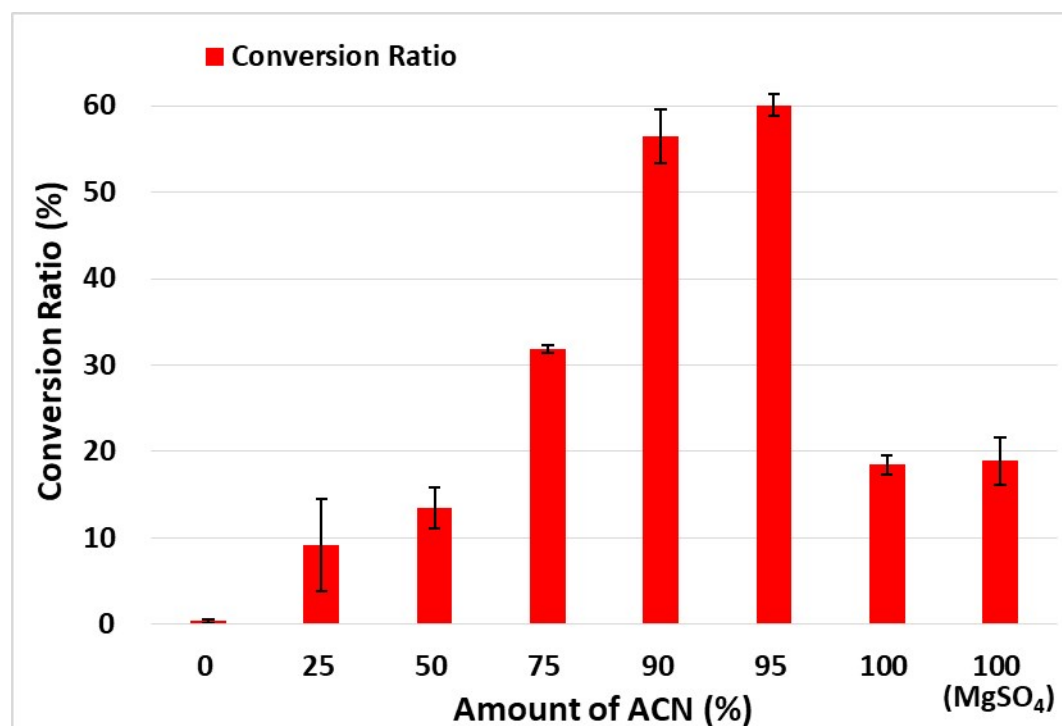


Figure S19. Effect of trace amounts of water Composition-dependent experiment using ACN with different percentages water for reactions of DBPA, with ionization by EESI and using carbon dioxide as nebulization gas.

6. Summary of droplet and bulk reactions

To compare reaction acceleration in microdroplets under different conditions, experiments were performed for microdroplet reactions and bulk reactions under a variety of conditions. nESI and ESSI were implemented for the microdroplet generation and reaction, and were also used to create the detected ions (Note that analysis of bulk reaction also involved the generation of microdroplets but this was done under non-accelerating conditions as described elsewhere).³ The carbon dioxide source can be room air CO₂ or external CO₂ provided from the interface by ESSI or from the solution. **Table S4** summarizes the information on the reaction and **Figure S20** summarizes the proposed mechanisms. Entries 1 to 4 are controls showing behavior in absence of an external CO₂ source. An initially surprising observation was product formation by simply spraying DBPA in solvent containing trace amounts of water. This demonstrates that the superacid proposed to be on the droplet surface makes room air CO₂ extremely reactive, so even the small amount of CO₂ in the atmosphere can react with amine in short times. Entry 5 to 8 show results of injecting CO₂ gas for 10 seconds followed by analysis by nESI or ESSI. Note that in these four experiments, CO₂ is in excess in the droplet and will diffuse to the surface for reaction during the analysis. Entry 5 and 7 show that the bulk reaction in ACN is slow, while entry 6 and 8 have higher conversion ratios. We rationalize this by reaction that occurs while analyzing the bulk reaction after injection of CO₂. The excess CO₂ in the droplet will diffuse to the surface of the droplet and the trace amounts of water in the droplet can further enhance the reactivity of CO₂ at the surface by surface protons (superacid at the surface). The data for these two reaction conditions strengthen the evidence for the role of trace water in droplet chemistry. Entries 9 and 10 show that the droplet reaction utilizing interfacial CO₂ is extremely fast compared to the bulk reaction. The conversion ratio can reach 30% on the millisecond timescale. Moreover, trace amounts of water enhance the conversion ratio to 60% presumably, again, by superacid at the interface of the droplet.

Table S4. Reaction of DBPA with carbon dioxide under different conditions

	Solvent	Method	Reaction Type	CR (%)	Time
1	ACN	nESI	N/A	0.00	N/A
2	95% ACN	nESI	N/A	0.32	N/A
3	ACN	ESSI (N ₂)	N/A	0.00	N/A
4	95% ACN	ESSI (N ₂)	N/A	0.83	N/A
5	ACN	Inject CO ₂ then nESI	Bulk + Droplet (solution CO ₂)	0.61	10 s + 1~10 ms
6	95% ACN	Inject CO ₂ then nESI	Bulk + Droplet (solution CO ₂)	14.07	10 s + 1~10 ms
7	ACN	Inject CO ₂ then ESSI (N ₂)	Bulk + Droplet (solution CO ₂)	1.96	10 s + 1~10 ms
8	95% ACN	Inject CO ₂ then ESSI (N ₂)	Bulk + Droplet (solution CO ₂)	32.20	10 s + 1~10 ms
9	ACN	ESSI (CO ₂)	Droplet (Interfacial CO ₂)	31.53	1~10 ms
10	95% ACN	ESSI (CO ₂)	Droplet (Interfacial CO ₂)	60.05	

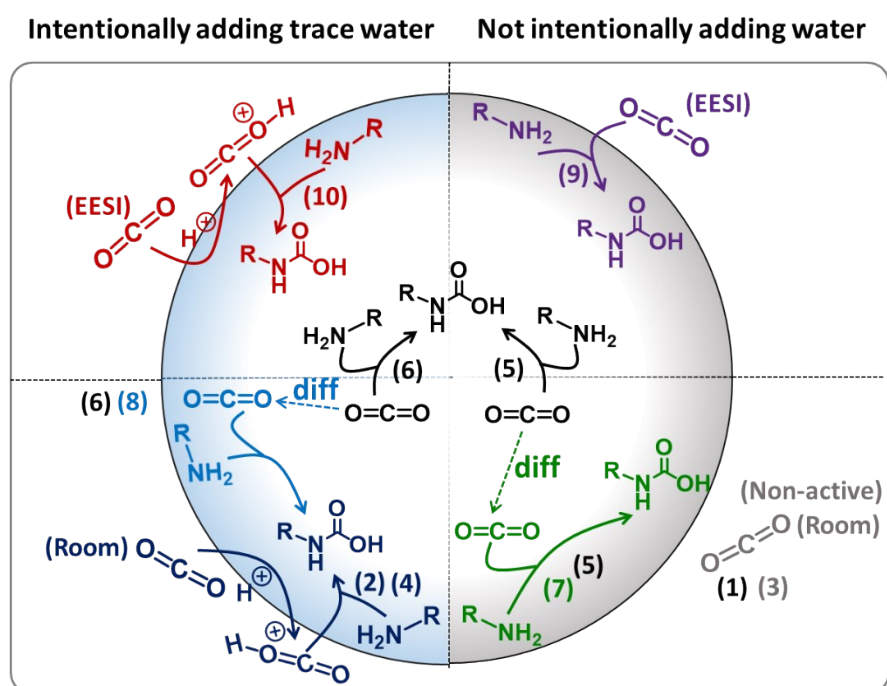


Figure S20. Reaction mechanism of microdroplet reactions for various conditions. The reaction mechanism were corresponding to the entry in **Table S4**.

7. The possibility of gas phase ion/molecule reactions

In this section we provide evidence that the carbonylation reaction occurs on the droplet surface, even though a referee has argued that the data could also allow a gas phase ion/molecule reaction. As a result, we conducted experiments to determine if it is possible that gas phase ion/molecule reactions played a significant role. Gas phase reactions could conceivably result from four processes which will be addressed in turn:

- (1) complete evaporation of solvent to produce charged amines
- (2) evaporation of volatile reagents into the gas phase where they react with CO₂
- (3) droplet fission (or direct ion evaporation) to generate gas phase ions that then undergo ion/molecule reactions with CO₂
- (4) desolvation of droplets in the MS inlet and subsequent ion/molecule reactions in the inlet.

Considering the issue of solvent evaporation, we note that the initial droplet size is estimated to be 3 - 6 μm^{4,5} and the droplet velocity is estimated as 60 -120 m/s,⁴⁻⁶ depending on the nebulizer gas pressure and sprayer aperture size. The distance between the sprayer and the inlet is normally 2 cm in our case, so we estimate the flight time of the droplets to be in the range 0.17- 0.33 ms. During this time, evaporation of solvent will occur and droplet fission may occur if the Rayleigh limit is reached. From a recent simulation of evaporation of methanol microdroplets,⁷ the smallest droplet (3 μm) when moving most slowly (60 m/s) will undergo evaporation to a size of 2.7 μm after 0.33 ms. The boiling point and vapor pressure of acetonitrile is much higher than that of methanol, so we conclude that during the timescale of our study, even the smallest initial microdroplet will have evaporated so little that the droplet diameter will be at least 2.7 μm.

To address the second possibility, that of evaporation of the amine reagent, we conducted CO₂ reactions with the reagent 2-aminoethyl trimethylammonium (ATA, structure shown in Figure S21). This salt should have a near-zero vapor pressure, however, we observed reaction with CO₂ to a similar extent (conversion ratio 45%) to that with the volatile amine dibutylaminopropylene diamine (conversion ratio 60 %). We also confirmed by MS/MS experiments that the product is a covalent bonded product instead of ion/molecule cluster. These results exclude significant contributions from vaporization of the amine reagents.

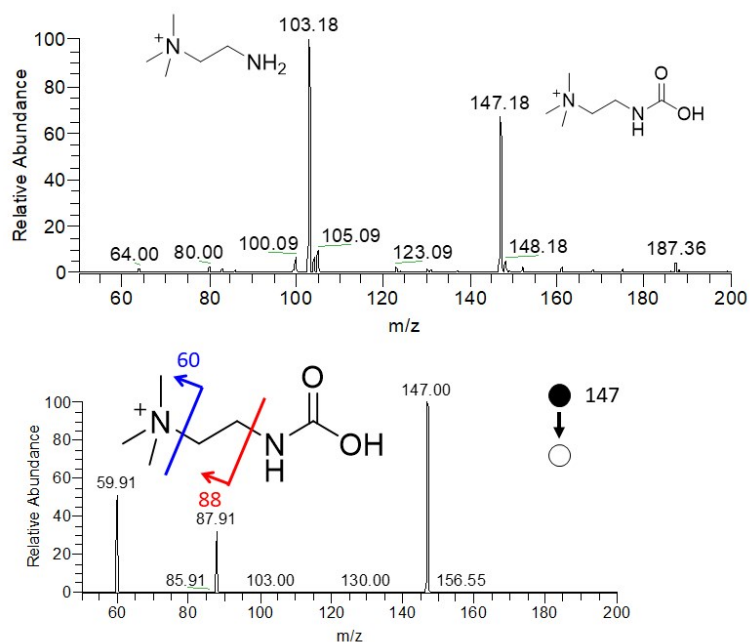


Figure S21. Reaction of ATA with CO₂ and the MS/MS for the product.

To address possibility (3), we start by considering that during droplet transfer coulombic fission can occur and generate much smaller offspring droplets. While it is difficult to estimate the degree of charging and hence the probability of fission, the smaller offspring droplets which will undergo rapid evaporation and generate gaseous ions. This reiterates the question of whether the observed reaction with CO₂ might be a gas phase ion/molecule reaction. We conducted new experiments which rule out any significant involvement of gas phase ion/molecule reactions by comparing droplet reactions with CO₂ to authentic ambient ion/molecule reactions between protonated amines and CO₂. The experimental setup is shown in the **Figure S22** below.

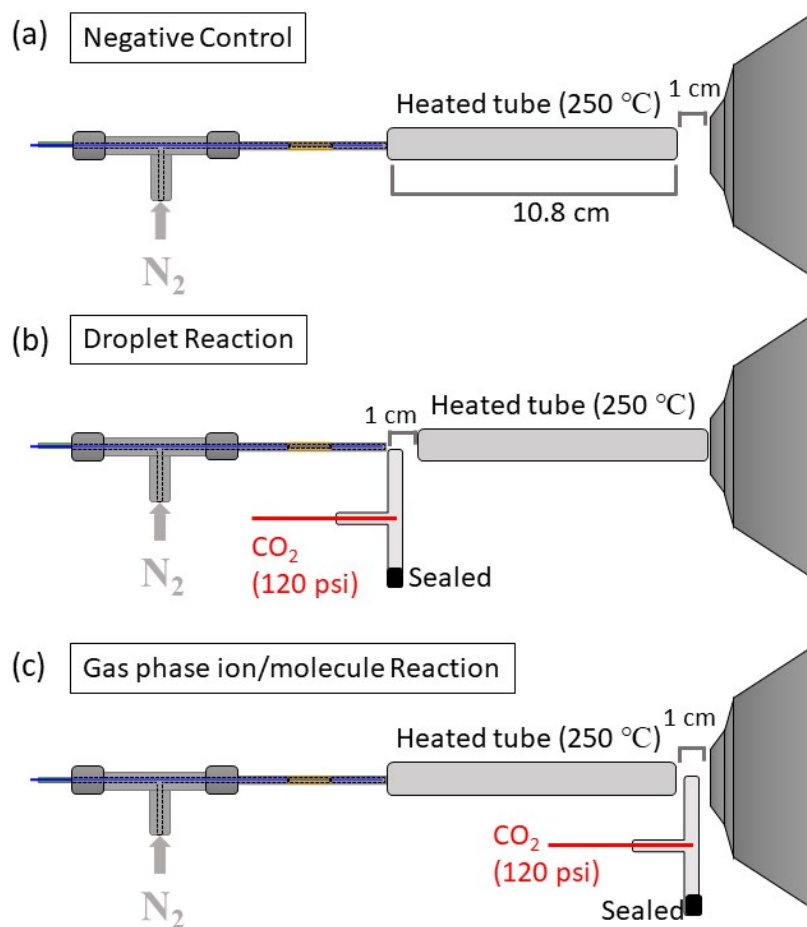


Figure S22. Experimental setup for (a) control experiment, (b) droplet reactions, and (c) gas phase ion/molecule reaction

Amine solution (10 μ M of DBPA in 95% ACN) was sprayed using N_2 nebulizing gas into a heating tube (250 °C, 10.8 cm) to perform complete desolvation. The data in **Figure S23** part (a) constitute a negative control. The data in parts (b) and (c) show the results of introducing gaseous CO_2 via a T-shaped glass tube before or after the heated desolvation tube. Introducing CO_2 before the heated tube (b) allows the droplet reaction, while introduction after the heated tube (c) only allows gas phase ion/molecule reactions. The data show that experiment (b) yielded carbamate while (c) gave virtually no product. This confirms that the reaction happens to an overwhelming extent with droplets. (Note that collisions of the nebulizing CO_2 gas with a 4 μ m amine droplet can give a high concentration of captured CO_2 on the time scale of the droplet transfer even if the trapping efficiency is low.)

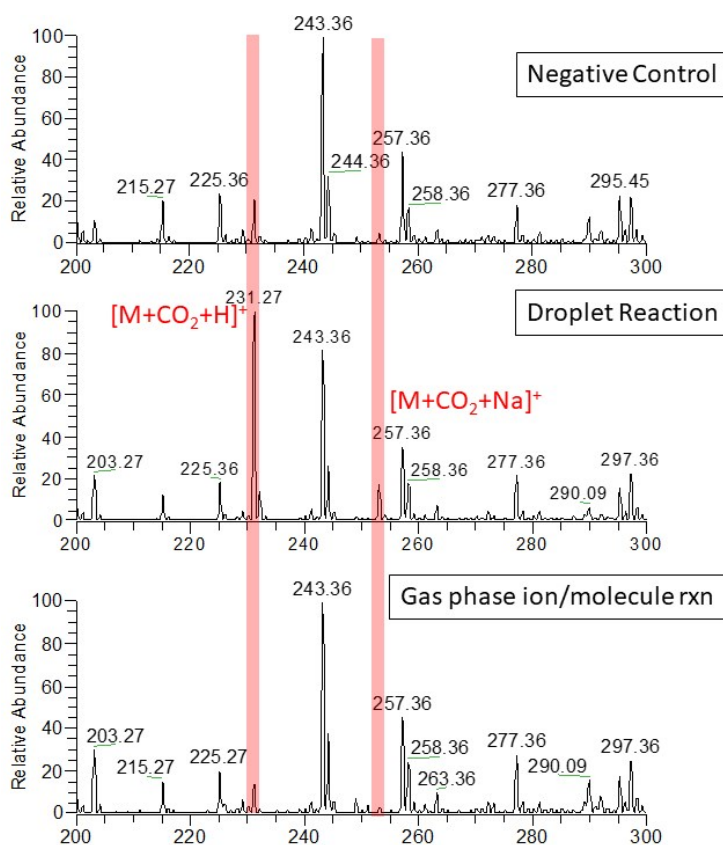


Figure S24. Spectra of Amine/CO₂ reaction in droplet and gas phase

To address the last possibility (4) that could result in ion/molecule reactions, we varied the inlet temperature from 50 °C to 250 °C, and collected the mass spectra continuously over this range of temperatures (for practical reasons, in segments). We found that the conversion ratio did not vary significant with the change of temperature, indicating that desolvation in the inlet is not significant. This result is consistent with an important previously stated conclusion for droplet reactions, namely that they undergo rapid, irreversible desolvation within the ion source.⁸

As a result of these considerations and experiments, we conclude that gaseous ion/molecule reactions can only make a minor contribution to carbamate formation when amine droplets react with CO₂.

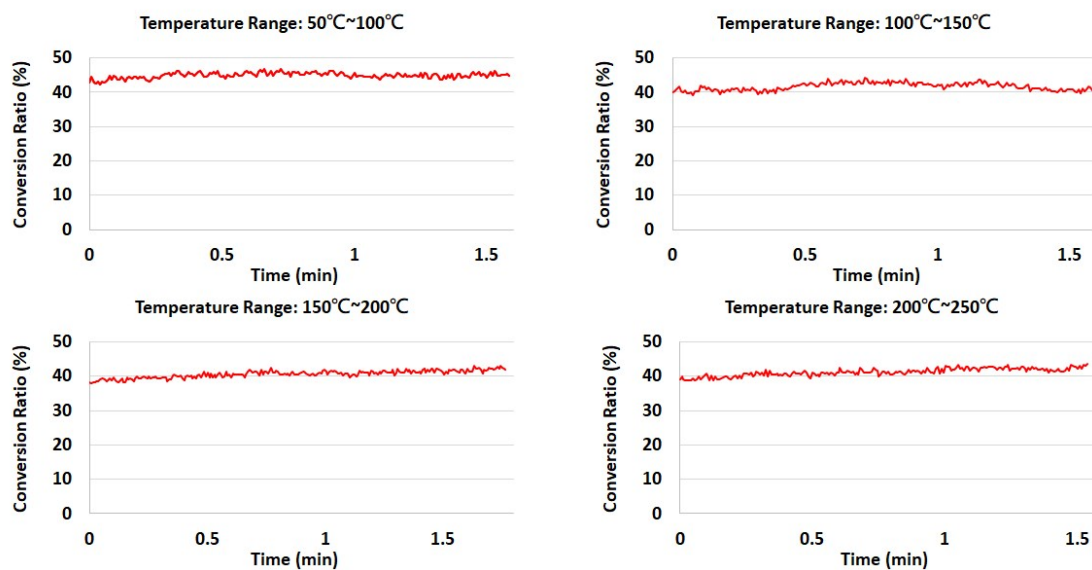


Figure S25. Temperature dependent experiment

8. References

1. "Study of the BMIM-PF6: acetonitrile binary mixture as a solvent for electrochemical studies involving CO₂." *Electrochim. Acta*, 2011, **56**, 5003-5009.
2. "Measurement and modeling of CO₂ diffusion coefficient in Saline Aquifer at reservoir conditions." *Cent. Eur. J. Eng.*, 2013, **3**, 585-594
3. "Accelerated Reaction Kinetics in Microdroplets: Overview and Recent Developments." *Annu. Rev. Phys. Chem.*, 2020, **71**, 31-51
4. "Droplet Dynamics and Ionization Mechanisms in Desorption Electrospray Ionization Mass Spectrometry." *Anal. Chem.*, 2006, **78**, 8549-8555
5. "Microdroplet fusion mass spectrometry for fast reaction kinetics." *Proc. Natl. Acad. Sci. USA*, **112**, 3898–3903
6. "Microdroplets Accelerate Ring Opening of Epoxides." *J. Am. Soc. Mass Spectrom.*, 2018, **29**, 1036-1043
7. "A kinetic description of how interfaces accelerate reactions in micro-compartments." *Chem. Sci.*, 2020,**11**, 8533-8545
8. "Organic Reactions in Microdroplets: Reaction Acceleration Revealed by Mass Spectrometry" *Angew. Chem. Int. Ed.*, 2016, **55**, 12960-12972.